Cellular signalling in abdominal aortic aneurysms

Groeneveld, M.E.

2020

PART II

CELLULAR SIGNALLING INFLUENCES ANEURYSM GROWTH AND RUPTURE

Chapter 5: Activation of Extracellular signal-Regulated Kinase in abdominal aortic aneurysm

Chapter 6: Update on Activation of Extracellular signal-Regulated Kinase in abdominal aortic aneurysm

Chapter 7: Betaglycan (TGFBR3) upregulation correlates with increased TGF-ß signalling in Marfan patient fibroblasts in vitro

CHAPTER 5

ACTIVATION OF EXTRACELLULAR SIGNAL-REGULATED KINASE IN ABDOMINAL AORTIC ANEURYSM

M.E. Groeneveld[1,2]
M.V. van Burink[1]
M.P.V. Begieneman[3,4]
H.W.M. Niessen[3]
W. Wisselink[1]
E.C. Eringa[2]
K.K. Yeung[1,2]

[1] Department of Vascular Surgery, Amsterdam University Medical Center
[2] Department of Physiology; Amsterdam University Medical Center
[3] Department of Pathology and Cardiac Surgery, Amsterdam University Medical Center
[4] Netherlands Forensic Institute, The Hague

European Journal of Clinical Investigation 2016, vol. 46, pag. 440–447

ABSTRACT

Objective: Extracellular matrix degeneration, caused by matrix metalloproteinase-2, facilitates smooth muscle cell migration leading to medial layer decline and, ultimately, abdominal aortic aneurysm. It remains unclear what exactly causes aneurysms to rupture, which leads to death in most patients. The extracellular signal-regulated kinase may be linked to the latter process. We aimed to clarify the role of extracellular signal-regulated kinase in aortic aneurysm development and rupture in patients.

Methods: Aortic fragments were harvested during open repair of non-ruptured (n=20) and ruptured (n=8) aneurysms. As control, non-dilated aortas (n=6) were obtained during autopsy. We determined levels of phosphorylated and total extracellular signal-regulated kinase by Western blot, matrix metalloproteinase-2 by immunohistochemistry, and medial layer thickness by conventional microscopy.

Results: Non-ruptured aneurysms had 1.8-times higher activation of extracellular signal-regulated kinase (ratio: phosphorylated/total) than controls ($p=0.011$). However, the ruptured aneurysms had only 0.9-times the activation of controls (ns). Both non-ruptured and ruptured aneurysms showed significantly higher matrix metalloproteinase-2 than controls (3.8 and 4.0-times, respectively; $p<0.005$). Of the medial layer thickness in controls the median was 1.5 mm, in non-ruptured 1.0 mm and in ruptured aneurysms 0.7 mm. Activation of extracellular signal-regulated kinase correlated positively to medial layer thickness ($Rs=0.48$; $p=0.014$), but not to matrix metalloproteinase-2 ($Rs=-0.36$; $p=0.10$).

Conclusions: In this study, non-ruptured aneurysms are associated with increased extracellular signal-regulated kinase activation while ruptured aneurysms are not. Extracellular signal-regulated kinase was not related to total matrix metalloproteinase-2 expression. We therefore speculate that increased extracellular signal-regulated kinase, in response to medial layer decline, could be protective against aneurysm rupture.

1. INTRODUCTION

Abdominal aortic aneurysm (AAA) development is caused by aortic medial layer degeneration. This is a multifactorial process featuring apoptosis of non-proliferating smooth muscle cells (SMC) and SMC migration from the medial to the intimal layer, facilitated via extracellular matrix (ECM) degradation by matrix metalloproteinases (MMP). These processes cause medial layer thinning, leading to AAA development and life threatening intra-abdominal bleeding in case of rupture.

A signalling pathway that may be involved in all aforementioned processes is extracellular signal-regulated kinase1/2 (ERK1/2).[1-2] ERK1/2 is one of four major mitogen-activated protein kinase signalling pathways that regulates aortic wall structure by stimulating proliferation and cell survival on one hand, and by activating SMC migration and apoptosis on the other.[3] It is stimulated by growth factors, cytokines and SMC damage.[4-5] In case of aortic wall inflammation or SMC damage, ERK1/2 stimulates SMC proliferation.[4,6] In contrast, ERK1/2 also stimulates ECM degradation, leading to SMC migration and medial layer decline.[1,7-8] ECM degradation is mainly performed by MMP-2 and -9.[7-8] MMPs are produced, among others, by SMC and infiltrating leukocytes.[9-10] In a rodent AAA model ERK1/2 was shown to be a critical regulator of MMP expression and Habashi e.a. concluded ERK1/2 to be a stimulating factor of rodent AAA development, as they demonstrated ERK1/2 inhibition to delay AAA growth. [11-12] In humans, ERK1/2 levels were demonstrated to be higher in patients who underwent elective surgical treatment of non-ruptured AAA as compared to healthy controls, and in human aortic SMC MMP-2 expression was regulated by ERK 1/2 activation.[11,13] However, ERK1/2 levels were never investigated in tissue of ruptured AAA.

We hypothesized that ERK1/2 and MMP-2 are higher in non-ruptured and ruptured AAA than in controls, with the highest levels in ruptured. Furthermore, we assessed whether ERK1/2 could be linked to factors of medial layer decline.

To test these hypotheses, we studied ERK1/2 in three groups: healthy aortas, non-ruptured AAA and ruptured AAA. Secondly, to examine if ERK1/2 is associated with key factors of AAA development, we investigated potential relationships with medial MMP-2 expression and medial layer thickness.

2. MATERIAL AND METHODS

The study was approved by the VU University Medical Center Medical Ethical Committee. Informed consent was obtained from all patients or family.

2.1 Patients and tissue collection

Aneurysm tissue was harvested from the ventral wall during open surgical repair of consecutively treated non-ruptured and ruptured AAA. The non-ruptured group consisted of 20 patients (15 men, median age 67 years) and the ruptured group of 8 patients (4 men, median age 74 years (table 5.1)). We also obtained ventral abdominal aortic tissue of 6 deceased patients (4 men, ages ranging from 51 – 71 years) at the start of autopsy, who had no AAA and no macroscopic atherosclerosis.

All tissues were snap frozen, cut in 5μm thick cryosections, air-dried and stored at -80˚C until use. Total leukocyte count, C-reactive protein and estimated glomerular filtration rate were measured by the department of clinical chemistry.

2.2 Western blot analysis

Western blotting of aortic samples was performed as described before.[14] Full thickness samples (i.e. intimal, medial and adventitial layer) of frozen tissue were used. Total and phosphorylated ERK1/2 (tERK1/2 and pERK1/2), the latter being the activated form, were quantified using AIDA software (Raytest, version 4.1.5). ERK1/2 activation was given as the ratio of pERK1/2 and tERK1/2.

2.3 Hematoxylin-Eosin staining

Cryosections were air-dried, fixed in 10% formalin and stained by hematoxylin-eosin staining. The medial layer was identified (representative image in figure 5.3A) and its thickness was measured using ImageJ software (National Institutes of Health, ImageJ, version 1.47).

2.4 Immunohistochemistry

Cryosections were stained for MMP-2 (Genetex; GTX27033; 1:100), visualized using 3,3'-diaminobenzidine (DAB) and counterstained with hematoxylin. PBS controls were included as negative control (all negative results, data not shown). Images were made as described above. MMP-2 levels in the medial layer were measured using ImageJ software by two independent observers in blinded fashion.

2.5 Statistical analysis

For continuous variables Kruskal–Wallis (multiple groups) and Mann–Whitney U (two groups) tests were used, Spearman's Rank (Rs) for correlations and Fisher's exact test for two groups with categorical variables (SPSS 20.0, USA). Boxplots with medians, interquartile ranges and outliers (Tukey's criteria) are given. Tests were considered statistically significant at p≤0.05.

Table 5.1 Baseline patient characteristics
Data are given for non-ruptured and ruptured AAA groups. P-values are given to compare both groups. Significant differences are indicated with an asterisk. Of four patients in the non-ruptured group C-reactive protein was not measured pre-operatively and the medication of one patient in the ruptured group was not known.

	Non-ruptured	**Ruptured**	***p***
N	20	8	
Male / female	15 / 5	4 / 4	0.371
Age *(years)*	67 (53 - 78)	74 (64 - 89)	0.067
Aneurysm diameter *(cm)*	5.6 (3.6 – 7.1)	8.0 (6.8 – 10.0)	0.045*
Smoking history *(%)*	65%	50%	0.671
Symptoms *(%)*	35%	100%	0.002*
Claudication (%)	*35%*	*0%*	0.008*
Backpain (%)	*0%*	*50%*	0.003*
Other (%)	*5%*	*50%*	0.015*
Coronary heart disease *(%)*	40%	63%	0.410
Hypertension *(%)*	75%	75%	1.000
Hypercholesterol *(%)*	35%	25%	1.000
COPD† *(%)*	30%	38%	1.000
Diabetes Mellitus *(%)*	15%	25%	0.606
Antihypertensives *(%)*	80%	75%	1.000
Statins*(%)*	40%	38%	1.000
Anticoagulants *(%)*	85%	63%	0.311
Leukocytes *(10^9/l)*	7.7 (3.3 – 11.1)	23 (13 - 30)	0.013*
C-reactive protein *(mg/l)*	2.5 (2.5 – 3.6; 37.7)	31 (8 - 124)	0.008*
eGFR‡ *(ml/min/1.73m^2)*	67 (49-90)	46 (21 - 55)	0.003*

*p ≤ 0.05; †COPD = chronic obstructive pulmonary disease; ‡ eGFR = estimated glomerular filtration.

3. RESULTS

3.1 Larger aneurysm diameter and systemic inflammation in ruptured AAA

In non-ruptured AAA median aneurysm diameter was 5.6 cm, while in ruptured AAA it was 8.0 cm (p=0.045; table 5.1). The non-ruptured group consisted of 1 supra-, 8 juxta- and 11 infra-renal AAA. In the ruptured group were 4 juxta- and 4 infra-renal AAA. For all below measured parameters no differences were found between these subgroups. One third of non-ruptured AAA patients suffered from symptoms, mainly claudication. In contrast all ruptured AAA patients suffered from symptoms, being back pain or other (p=0.002).

Median total leukocyte count and C-reactive protein (normal range values used by our clinical chemistry department are $<10*10^9$/l and <5 mg/l, respectively) were markedly and significantly increased in ruptured AAA ($23*10^9$ and 31 mg/ml, respectively; table 5.1) as compared to non-ruptured AAA ($7.7*10^9$ and 2.5 mg/ml, p=0.013 and p=0.008, respectively). Estimated glomerular filtration rate was 67 ml/min/1.73m^2 in non-ruptured AAA and was declined significantly in ruptured AAA to 46 ml/min/1.73m^2 (p=0.003).

3.2 ERK1/2 levels were highest in non-ruptured AAA

Median pERK1/2 and median ERK1/2 activation (ratio of pERK1/2 and tERK1/2) were highest in non-ruptured AAA. Levels were increased 5.0 and 1.8-times, respectively, as compared to controls and 11.1 and 2.0-times, respectively, as compared to ruptured AAA (pERK1/2: p≤0.011, figure 5.1B; ERK1/2 activation: p≤0.022, figure 5.1C). The highest levels of tERK1/2 were found in non-ruptured AAA, however, no statistically significant differences in tERK1/2 were found when compared to controls and ruptured AAA (p=0.191 and p=0.075, respectively; see figure 5.1A).

3.3 MMP-2 levels increased in both ruptured and non-ruptured AAA

In controls MMP-2 showed weak staining in the medial layer (figure 5.2A). In non-ruptured AAA MMP-2 was markedly increased compared to controls and was localized mainly in the medial layer centre in well-defined circular areas (figure 5.2B). In ruptured AAA a global MMP-2 staining was seen throughout the medial layer, collected in well-defined circular areas as well (figure 5.2C). Quantification of MMP-2 expression showed that in both non-ruptured and ruptured AAA MMP-2 expression was higher than in controls. The highest levels of MMP-2 were found in ruptured AAA followed by non-ruptured (4.0 and 3.8 times higher than controls, p=0.004 and p=0.001, respectively, figure 5.2D), albeit not significantly.

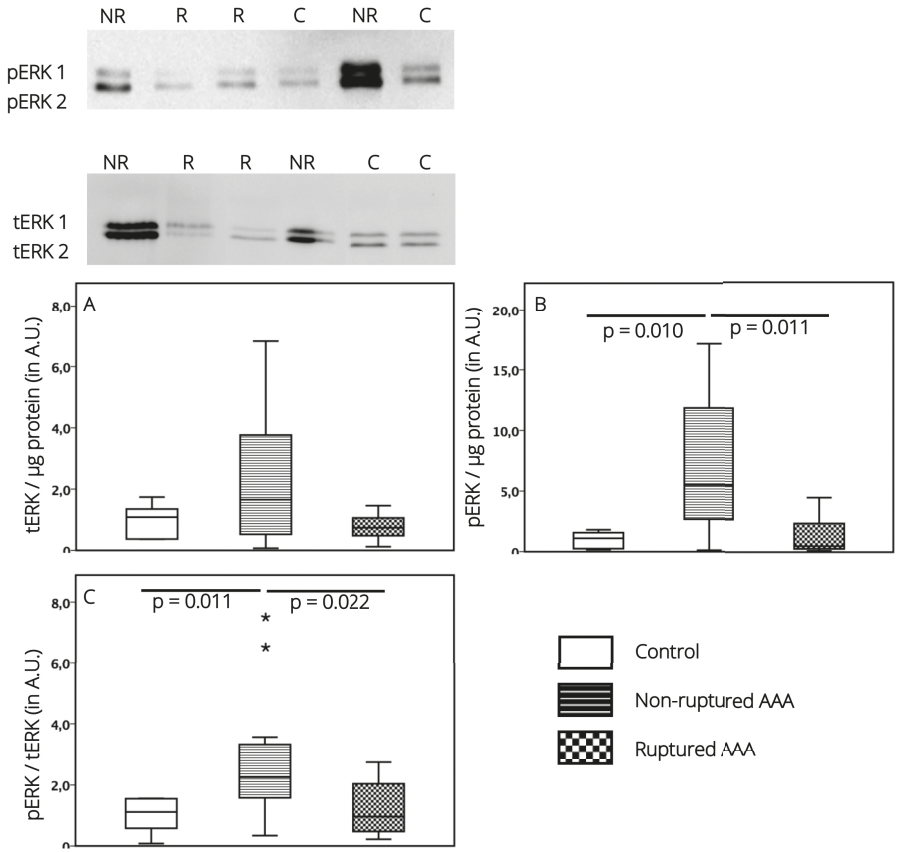

Figure 5.1 ERK1/2 signalling in healthy aorta, non-ruptured and ruptured AAA
Examples of western blot analysis of tERK1/2 and pERK1/2 are seen above. Concentrations of tERK1/2 (A), pERK1/2 (B) and ratio of pERK1/2 and tERK1/2 (C) as an indication of ERK1/2 activation are given in the graphs underneath. Data are presented as boxplots with interquartile ranges. Outliers are indicated by an asterisk. ERK1/2 per µg tissue is given in arbitrary units (A.U.). Statistically significant differences are given with p-values below the horizontal bar.

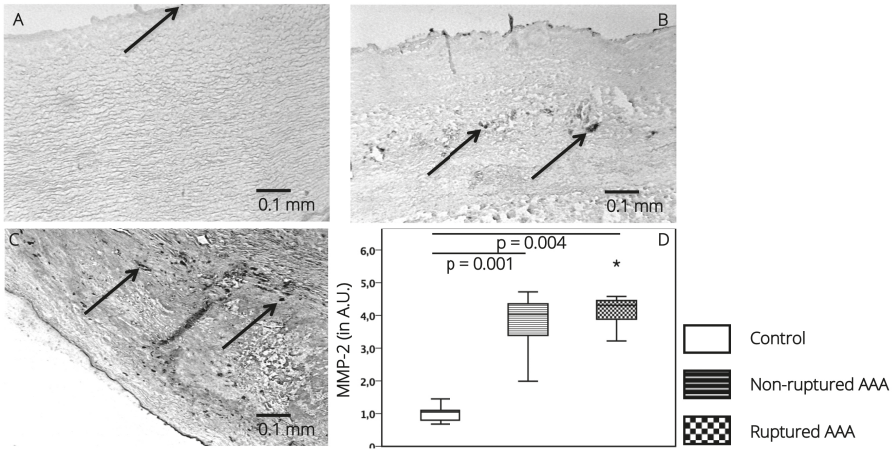

Figure 5.2 MMP-2 expression in healthy aorta, non-ruptured and ruptured AAA
In figures A, B and C representative images of MMP-2 expression in the medial layer are given of healthy aorta, non-ruptured AAA and ruptured AAA, respectively. Black staining in the images indicates MMP-2 expression (see arrows). Pictures were made using a 20X objective. In figure D the amounts of MMP-2, measured in the medial layer by immunohistochemistry staining, are given in arbitrary units (A.U.). Data are presented as boxplots with interquartile ranges. Outliers are indicated by an asterisk. Statistically significant differences are given with p-values below the horizontal bar.

3.4 Medial layer thickness declined in ruptured AAA

In healthy control aorta the medial layer comprises the greater part of the vessel wall and the collagen fibres, as can be seen in figure 5.2A, are organised in regular patterns; the median medial layer thickness was 1.5 mm (figure 5.3B). In non-ruptured AAA the median medial layer thickness was declined and the regular pattern of collagen fibres was disturbed (figure 5.2B). Median medial layer was 1.0 mm thick (figure 5.3B) and covered a smaller part of the total vessel wall than in controls, due to decreased medial layer thickness and an increased intimal layer thickness. In ruptured AAA the medial layer thickness further declined and the regular pattern of collagen fibres was disrupted (figure 5.2C and 5.3A). Median medial layer thickness in ruptured AAA was 0.7 mm (figure 5.3B). Controls had a 2.0-times thicker medial layer than ruptured AAA (p=0.019, figure 5.3B). No significant differences existed between non-ruptured and ruptured AAA, or between non-ruptured AAA and controls.

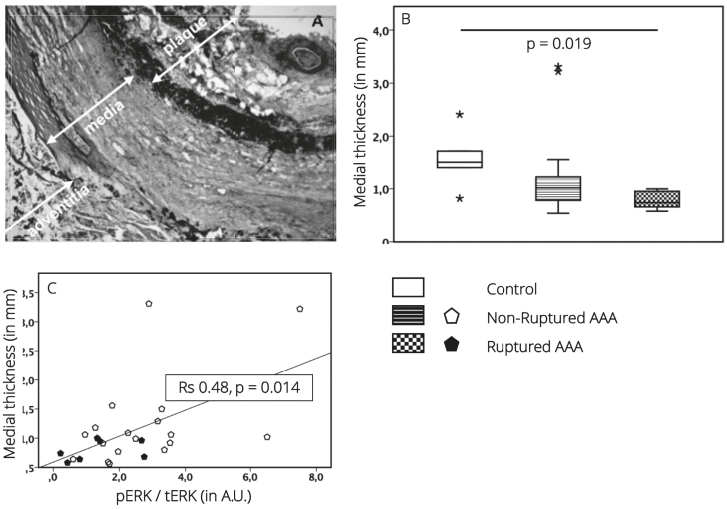

Figure 5.3 Medial layer thickness and association with ERK1/2 signalling
A representative image of a ruptured AAA stained by hematoxylin-eosin is given in figure A (20X objective). The three separate layers are indicated, from lumen outwards: atherosclerotic plaque, medial layer and adventitial layer. Thickness of the medial layer in millimetres (mm) are presented as boxplots with interquartile ranges in figure B. Outliers are indicated by an asterisk. Statistically significant differences are given with p-values below the horizontal bar. In the graphs below, the correlations between ERK1/2 activation, given as ratio of pERK1/2 and tERK1/2 in arbitrary units (A.U.), and the aortic medial thickness (in mm) are presented for non-ruptured and ruptured AAA pooled (figure C). A line of best fit is drawn. The correlation is given as a Spearmans Rank (Rs) with p-value.

3.5 ERK1/2 is associated with medial layer thickness and circulating leukocytes but not with MMP-2 expression.

Sub-group analysis showed a positive association between the medial layer thickness and ERK1/2 activation in non-ruptured and ruptured AAA groups pooled (Rs 0.48; p=0.014 figure 5.3C). AAA patients with the highest ERK1/2 signalling retained the thickest medial layer. There was no such correlation found for MMP-2 expression and medial thickness (Rs -0.02; p=0.929).

As ERK1/2 is supposed to stimulate MMP-2 expression, we investigated a possible correlation between MMP-2 expression in the medial layer and levels of pERK1/2, tERK1/2 or ERK1/2 activation in the total vessel wall.[9] We found a trend towards association between ERK1/2 activation and MMP-2 (Rs -0.36; p=0.099). Total circulating leukocyte counts were negatively correlated with pERK1/2 and ERK1/2 activation in the vessel wall (Rs-0.63; p≤0.017), and as well with medial thickness (Rs -0.61; p=0.02). No correlation existed between circulating leukocytes and MMP-2 expression (Rs

0.38; p=0.23). Estimated glomerular filtration rate was positively correlated to ERK1/2 activation in the vessel wall (Rs 0.70; p=0.005).

4. DISCUSSION

The major findings of our study are: I) pERK1/2 and ERK1/2 activation are higher in non-ruptured AAA than in ruptured AAA and control tissue; II) ERK1/2 activation is positively associated with medial layer thickness in dilated aortas; III) in contrary to what was earlier described in rodent models, no association exists between ERK1/2 and MMP-2 expression in human AAA medial layer.

In our study, we demonstrated that levels of pERK1/2 and ERK1/2 activation are significantly higher in non-ruptured AAA than in ruptured. Interestingly, ERK1/2 activation in ruptured AAA is similar to that in controls. This observation could be explained by the fact that aortic SMC are responsible for ERK1/2 production and activation. In the developing aneurysm SMC are known to migrate from the medial to the intimal layer where they go into apoptosis.[15-17] Increased migration and apoptosis cause decreased SMC numbers and consequently medial layer thinning. We found that medial thickness declines as the healthy aorta develops from a non-ruptured to a ruptured AAA. In AAA patients, we found that pERK1/2 and ERK1/2 activation were positively correlated with medial thickness. This association means that when ERK1/2 levels decrease, the medial thickness declines and vice versa. It could be explained, as suggested above, that ERK1/2 is produced and activated by SMC in the aortic aneurysm wall. Consequently, when the aneurysm develops the medial thickness declines and less SMC remain to keep up the production of ERK1/2 levels. Or, on the other hand, medial thickness is preserved as long as ERK1/2 levels are high, due to SMC proliferation by ERK1/2 signalling.[18] When ERK1/2 levels decrease, as is the case in ruptured AAA, the medial layer is no longer capable to reactively proliferate SMC and eventually becomes thinner.

AAA formation is characterised by ECM degradation and medial layer destruction. The medial layer becomes thinner and the aortic diameter increases. MMP are enzymes that traditionally are known for ECM degradation in the vessel wall. However, recently MMP-2 was demonstrated to be not only responsible for ECM degradation but for ECM proliferation as well, by stimulating collagen and elastin production.[19] In earlier studies mainly MMP-2 and -9 have increased activity in the vessel wall of aortic aneurysms and could be related to aneurysm size and rupture.[20] As mentioned above, MMP-2

and -9 expression are thought to be regulated by ERK1/2 and delay AAA growth by ERK 1/2 inhibition.[12,21] To verify these hypotheses for human AAA we measured MMP-2 expression in the medial layer of patients and controls. Our data show an increased MMP-2 expression in the non-ruptured and ruptured AAA as compared to healthy aorta. ERK1/2 levels are high in non-ruptured AAA but not in ruptured, and MMP-2 expression is not associated with ERK1/2. This lack of association can be explained by the recently discovered divergent role of MMP-2, providing evidence that MMP-2 expression in the aneurysm wall is not only associated with aortic degeneration but with ECM repair and synthesis as well.[19] However, we hypothesize that in human aortic SMC MMP-2 expression can be regulated by ERK1/2 signalling, but as an association lacks it is probably not responsible for total MMP-2 expression. Therefore we suggest that MMP-2 expression, as opposed to earlier findings in rodent studies, is not fully dependant on ERK1/2 stimulation and there should be another source of MMP-2.

Based on previous studies and our recent findings we suggest that aneurysm development initiates with inflammation of the aortic wall where factors of inflammation stimulate ERK1/2 signalling to induce SMC proliferation.[22-24] Consequently MMP-2 expression rises and the medial ECM will be enzymatically degraded (figure 5.4). This degradation facilitates SMC to migrate.[22,25] SMC migration and apoptosis might decrease the total amount of SMC and so total ERK1/2 signalling declines. This might explain the lower ERK1/2 levels in ruptured AAA . However, this does still not clarify the increased MMP-2 levels we found in both non-ruptured and ruptured AAA. Locally infiltrating leukocytes could be a possible alternative source of MMP-2. In ruptured AAA the total amount of circulating leukocytes was higher than in non-ruptured, and were negatively correlated to ERK1/2 activity. However, with our available data we could not investigate a possible association between total locally infiltrated leukocytes and ERK1/2 signalling. Therefore we can only speculate that, due to increased ERK1/2 signalling in the inflammatory aorta, vascular cell adhesion molecule-1 is overexpressed and augments leukocyte infiltration in the vessel wall.[26-27] As leukocytes, particularly neutrophils, are a known source of MMP-2 expression we suggest that leukocytes in the AAA wall could be responsible for the increasing MMP-2 levels, rather than SMC via ERK1/2 signalling.[28] This hypothesis is in part supported by our finding that in ruptured AAA patients we found higher circulating leukocyte counts in the blood than in non-ruptured AAA.

Two limitations of the present study should be considered. First, we could only include the ventral wall of the aneurysm, while rupture of the wall often occurs in the dorsal part of the aorta. However, as all the included aneurysms were fusiform one may

assume that the pathogenic process affects the aorta circularly, even if one takes the heterogeneity of the aneurysmal disease into account. Therefore we consider the specimens representative of the aneurysmatic aortic wall. Second, our conclusions are based on observational ex-vivo research. Further research in the role of ERK1/2 in inflammation of the aorta leading to SMC dysfunction and ECM degradation in aneurysm development is warranted. This might be performed by in-vitro experiments using SMC cultures to determine whether ERK1/2 provides protection against apoptosis.

In summary, the findings of the present study demonstrate for the first time that ERK1/2 activation in the medial layer of human aortas is higher in non-ruptured AAA than in ruptured AAA. Furthermore, ERK1/2 activation might be involved in preserving medial layer thickness, however, this is not regulated by MMP-2 expression. We suggest that in response to damage of the medial layer, ERK1/2 signalling performs a protective role against ECM degradation and, contrary to conclusions from earlier rodent studies, reduces medial layer decline and AAA rupture.

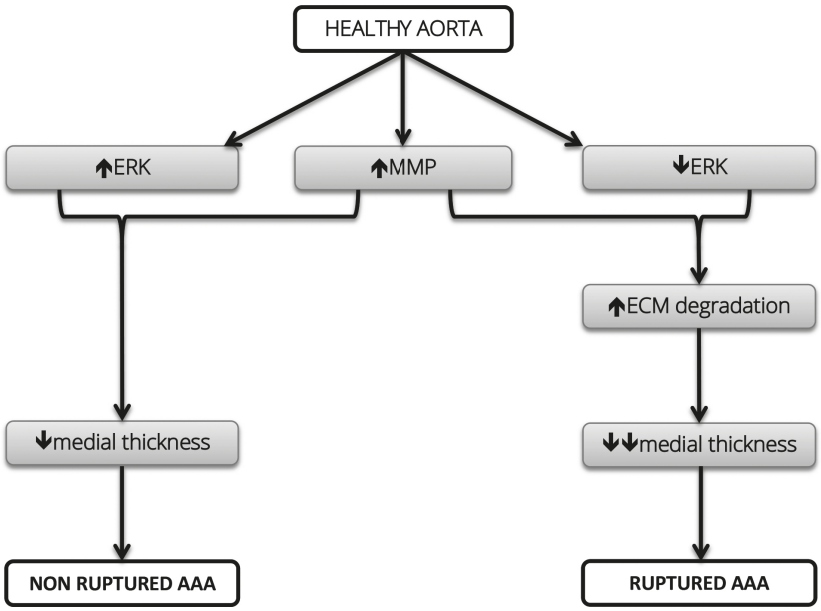

Figure 5.4 Model of aorta wall degeneration in AAA
The multifactorial process of AAA development initiates with inflammation of the aortic wall. ERK1/2 signalling potentially has both an active as a reactive role in an inflammatory environment. In this model we simplified the process of aortic wall degeneration leading to aneurysm development and rupture. One should keep into account that individual steps can be influenced by more factors than those implemented in this model. In non-ruptured AAA we measured increased MMP-2 expression as well as increased ERK1/2 activity, when compared to healthy controls. In ruptured AAA MMP-2 expression was increased, but ERK1/2 activity was not when compared to controls. ERK1/2 activity was positively associated with medial layer thickness in non-ruptured and ruptured AAA. We suggest that the increased ERK1/2 activity in non-ruptured AAA might be protective against AAA rupture.

REFERENCES

1. Nelson PR, Yamamura S, Mureebe L, Itoh H, Kent KC. Smooth muscle cell migration and proliferation are mediated by distinct phases of activation of the intracellular messenger mitogen-activated protein kinase. J Vasc Surg 1998; 27:117-25.
2. Chen Z, Cai Y, Zhang W, Liu X, Liu S. Astragaloside IV inhibits platelet-derived growth factor-BB-stimulated proliferation and migration of vascular smooth muscle cells via the inhibition of p38 MAPK signalling. Exp Ther Med. 2014 Oct;8(4):1253-1258.
3. Le Gall M, Chambard JC, Breittmayer JP, Grall D, Pouysségur J, Van Obberghen-Schilling E. The p42/p44 MAP Kinase Pathway Prevents Apoptosis Induced by Anchorage and Serum Removal. Mol Biol Cell. 2000 Mar;11(3):1103-12.
4. Koyama H, Olson NE, Dast van FF, Reidy MA. Cell Replication in the Arterial Wall Activation of Signaling Pathway Following In Vivo Injury. Circ Res. 1998;82:713-721.
5. Katz M, Amit I, Yarden Y. Regulation of MAPKs by growth factors and receptor tyrosine kinases. Biochim Biophys Acta. 2007 Aug;1773(8):1161-76.
6. Lu Z, Xu S., ERK1/2 MAP Kinases in Cell Survival and Apoptosis. IUBMB Life. 2006 Nov;58(11):621-31.
7. Palombo D, Maione M, Cifiello BI, Udini M, Maggio D, Lupo M. Matrix metalloproteinases. Their role in degenerative chronic diseases of abdominal aorta. J Cardiovasc Surg (Torino). 1999 Apr;40(2):257-60.
8. Longo GM, Xiong W, Greiner TC, Zhao Y, Fiotti N, Baxter BT. Matrix metalloproteinases 2 and 9 work in concert to produce aortic aneurysms. J Clin Invest. 2002 Sep;110(5):625-32.
9. Ferrans VJ.New insights into the world of matrix metalloproteinases. Circulation. 2002 Jan 29;105(4):405-7.
10. Reeps C, Pelisek J, Seidl S, Schuster T, Zimmermann A, Kuehnl A, Eckstein HH. Inflammatory infiltrates and neovessels are relevant sources of MMPs in abdominal aortic aneurysm wall. Pathobiology. 2009;76(5):243-52.
11. Ghosh A, DiMusto PD, Ehrlichman LK, Sadiq O, McEnvoy B, Futchko FS, Henke PK, Eliason JL, Upchurch GR. The role of Extracellular Signal Related Kinase during abdominal aortic aneurysm formation. J Am Coll Surg. 2012 Nov;215(5):668-680.
12. Habashi JP, Doyle JJ, Holm TM, Aziz H, Schoenhoff F, Bedja D, Chen Y, Modiri AN, Judge DP, Dietz HC. Angiotensin II Type 2 Receptor Signaling Attenuates Aortic Aneurysm in Mice Through ERK Antagonism. Science. 2011 Apr 15;332(6027):361-5.
13. Wang C, Qian X, Sun X, Chang Q. Angiotensin II increases matrix metallaproteinase 2 expression in human aortic smooth muscle cells via AT1R and ERK 1/2. Exp Biol Med (Maywood). 2015 Mar 11.
14. Eringa EC, Stehouwer CDA, Nieuw Amerongen GP, Ouwehand L, Westerhof N, Sipkema P. Vasoconstrictor effects of insulin in skeletal muscle arterioles are mediated by ERK1/2 activation in endothelium. Am J Physiol Heart Circ Physiol. 2004;287:H2043–H2048.
15. Goodall S, Porter KE, Bell PR, Thompson MM. Enhanced invasive properties exhibited by smooth muscle cells are associated with elevated production of MMP-2 in patients with aortic aneurysms. Eur J Vasc Endovasc Surg. 2002 Jul;24(1):72-80.

16. López-Candales A, Holmes DR, Liao S, Scott MJ, Wickline SA, Thompson RW. Decreased vascular smooth muscle cell density in medial degeneration of human abdominal aortic aneurysms. Am J Pathol. 1997 Mar;150(3):993-1007.

17. Thompson RW, Liao S, Curci JA. Vascular smooth muscle cell apoptosis in abdominal aortic aneurysms. Coron Artery Dis. 1997 Oct;8(10):623-31.

18. Isenovic ER, Trpkovic A, Zakula Z, Koricanac G, Marche P Role of ERK1/2 Activation In Thrombin-Induced Vascular Smooth Muscle Cell Hypertrophy. Current Hypertension Reviews, 2016; 4(3): 190-196.

19. Shen M, Lee J, Basu R, Sakamuri SS, Wang X, Fan D, Kassiri Z. Divergent roles of matrix metalloproteinase 2 in pathogenesis of thoracic aortic aneurysm. Arterioscler Thromb Vasc Biol. 2015;35:888-898.

20. Petersen E, Gineitis A, Wågberg F, Angquist KA. Activity of Matrix Metalloproteinase-2 and -9 in Abdominal Aortic Aneurysms. Relation to Size and Rupture. Eur J Vasc Endovasc Surg 20, 457–461 (2000).

21. Chakraborti S, Mandal M, Das S, Mandal A, Chakraborti T. Regulation of matrix metalloproteinases: an overview. Mol Cell Biochem. 2003 Nov;253(1-2):269-85.

22. Watanabe A, Ichiki T, Sankoda C, Takahara Y, Ikeda J, Inoue E, Tokunou T, Kitamoto S, Sunagawa K. Suppression of abdominal aortic aneurysm formation by inhibition of prolyl hydroxylase domain protein through attenuation of inflammation and extracellular matrix disruption. Clin Sci (Lond). 2014 May;126(9):671-8.

23. Ghoshal S, Loftin CD. Cyclooxygenase-2 inhibition attenuates abdominal aortic aneurysm progression in hyperlipidemic mice. PloS One. 2012;7(11).

24. Wang X, Liu JZ, Hu JX, Wu H, Li YL, Chen HL, Bai H, Hai CX. ROS-activated p38 MAPK/ERK-Akt cascade plays a central role in palmitic acid-stimulated hepatocyte proliferation. Free Radic Biol Med. 2011 Jul 15;51(2):539-51.

25. Thompson RW, Parks WC. Role of matrix metalloproteinases in abdominal aortic aneurysms. Ann N Y Acad Sci. 1996 Nov 18;800:157-74.

26. Rui W, Guan L, Zhang F, Zhang W, Ding W. PM2.5 -induced oxidative stress increases adhesion molecules expression in human endothelial cells through the ERK/AKT/NF-κB-dependent pathway. J Appl Toxicol. 2015 Apr 15.

27. Liu J, Wang Y, Ouyang X. Beyond toll-like receptors: Porphyromonas gingivalis induces IL-6, IL-8, and VCAM-1 expression through NOD-mediated NF-κB and ERK signaling pathways in periodontal fibroblasts. Inflammation. 2014 Apr;37(2):522-33.

28. Fontaine V, Jacob MP, Houard X, Rossignol P, Plissonnier D, Angles-Cano E, Michel JB. Involvement of the mural thrombus as a site of protease release and activation in human aortic aneurysms. Am J Pathol. 2002; 161: 1701–1710.

CHAPTER 6

UPDATE ON ACTIVATION OF EXTRACELLULAR SIGNAL-REGULATED KINASE IN ABDOMINAL AORTIC ANEURYSM

M.E. Groeneveld[1,2]
K.K. Yeung[1,2]

[1] Department of Vascular Surgery, Amsterdam University Medical Center
[2] Amsterdam Cardiovascular Sciences, Amsterdam University Medical Center

European Journal of Clinical Investigation 2018 Aug 12:e13016

Update on literature

Extracellular signal-regulated kinase (ERK) activation is associated with aortic aneurysm (AA) development and is enhanced in nonruptured AA.[1] ERK is a signalling protein responsible for aortic wall maintenance by vascular smooth muscle cell (VSMC) proliferation and migration.

When ERK activation is inhibited, it can reduce the inflammatory response in VSMC and eventually reduces AAA development.[2,3] When ERK activation was blocked in TGBR1 deficient mice, aneurysmal degeneration was prevented.[4]

Increased ERK activation in rats leads to enhanced aortic VSMC contractility resulting in hypertension and eventually cardiovascular disease like AAA.[5] However, in our unpublished pilot-studies, we measured impaired VSMC contractility in sporadic AAA and demonstrated a correlation between AAA growth rate in vivo versus contractility in vitro. The correlation of VSMC contraction with ERK-pathway is now still under investigation.

The above mentioned findings suggest that ERK has a deteriorating effect, rather than a protective role in AAA development.

Update on statements from: Activation of extracellular signal-related kinase in abdominal aortic aneurysm[1]

Statement 1: "Nonruptured aneurysms are associated with increased extracellular signal-regulated kinase activation while ruptured aneurysms are not"

The evidence that has accumulated in the meanwhile enforces this statement as stated above in the update.

Statement 2: "Extracellular signal-regulated kinase was not related to total matrix metalloproteinase-2 expression"

The evidence that has accumulated in the meanwhile weakens this statement. There are increasing signs that ERK activation and MMP expression are related.

REFERENCES

1. Groeneveld ME, van Burink MV, Begieneman MPV, et al. Activation of extracellular signal-related kinase in abdominal aortic aneurysm. *Eur J Clin Invest*. 2016;46(5). doi:10.1111/eci.12618.
2. Hao Q, Dong X, Chen X, et al. ACE2 Inhibits Angiotensin II-Induced Abdominal Aortic Aneurysm in Mice. *Hum Gene Ther*. 2017:hum.2016.144. doi:10.1089/hum.2016.144.
3. Yu M, Chen C, Cao Y, Qi R. Inhibitory effects of doxycycline on the onset and progression of abdominal aortic aneurysm and its related mechanisms. *Eur J Pharmacol*. 2017;811:101-109. doi:10.1016/j.ejphar.2017.05.041.
4. Yang P, Schmit BM, Fu C, et al. Smooth muscle cell-specific Tgfbr1 deficiency promotes aortic aneurysm formation by stimulating multiple signaling events. *Sci Rep*. 2016;6(September):1-15. doi:10.1038/srep35444.
5. Zhao Z, Wang J, Huo Z, Wang Z, Mei Q. FTY720 elevates smooth muscle contraction of aorta and blood pressure in rats via ERK activation. *Pharmacol Res Perspect*. 2017;5(3):e00308. doi:10.1002/prp2.308.

CHAPTER 7

BETAGLYCAN (TGFBR3) UPREGULATION CORRELATES WITH INCREASED TGF-ß SIGNALLING IN MARFAN PATIENT FIBROBLASTS IN VITRO

M.E. Groeneveld[1,2]
N. Bogunovic[1,2]
R.J.P. Musters[2]
G.J. Tangelder[2]
D. Micha[3]
W. Wisselink[1]
G. Pals[3]
K.K. Yeung[1,2]

[1] Department of Vascular Surgery, Amsterdam University Medical Center
[2] Department of Physiology, Amsterdam University Medical Center
[3] Department of Clinical Genetics, Amsterdam University Medical Center

Cardiovascular Pathology 2018 Jan – Feb, vol. 32, pag. 44-49

ABSTRACT

Background: Marfan syndrome (MFS), a congenital connective tissue disorder leading to aortic aneurysm development, is caused by fibrillin-1 (FBN1) gene mutations. Transforming growth factor beta (TGF-ß) might play a role in the pathogenesis. It is still a matter of discussion if and how TGF-ß upregulates the intracellular downstream pathway, although TGF-ß receptor 3 (TGFBR3 or Betaglycan) is thought to be involved. We aimed to elucidate the role of TGFBR3 protein in TGF-ß signaling in Marfan patients.

Methods: Dermal fibroblasts of MFS patients with haploinsufficient (HI; n=9) or dominant negative (DN; n=4) *FBN1* gene mutations, leading to insufficient or malfunctioning fibrillin-1, respectively, were used. Control cells (n=10) were from healthy volunteers. We quantified TGFBR3 protein expression by immunofluorescence microscopy and gene expression of *FBN1*, *TGFB1*, its receptors and downstream transcriptional target genes by quantitative PCR.

Results: Betaglycan protein expression in *FBN1* mutants pooled was higher than in controls (p=0.004) and in DN higher than in HI (p=0.015). In DN significant higher mRNA expression of *FBN1* (p=0.014), *SMAD7* (p=0.019), *HSP47* (p=0.023) and *SERPINE1* (p=0.008) was observed than in HI, but lower *HSPA5* expression (p=0.029). A pattern of higher expression was noted for *TGFB1* (p=0.059), *FN1* (p=0.089) and *COL1A1* (p=0.089) in DN as compared to HI. TGFBR3 protein expression in cells, both presence in the endoplasmic reticulum and amount of vesicles per cell, correlated positively with *TGFB1* mRNA expression (Rs=0.60, p=0.017; Rs=0.55, p=0.029; respectively). *TGFBR3* gene expression did not differ between groups.

Conclusion: We demonstrated that activation of TGF-ß signaling is higher in patients with a DN than a HI *FBN1* gene mutation. Also, TGFBR3 protein expression is increased in the DN group and correlates positively with *TGFB1* expression in groups pooled. We suggest that TGFBR3 protein expression is involved in upregulated TGF-ß signaling in MFS patients with a DN *FBN1* gene mutation.

1. INTRODUCTION

Marfan syndrome (MFS) is a connective tissue disorder that is characterized by abnormalities in the skeletal, ocular, pulmonary, nervous and cardiovascular system.[1–3] The most severe cardiovascular manifestation of MFS is the development of aortic aneurysms (AA), predominantly thoracic AA, which can lead to rupture associated with high mortality.[4,5] The syndrome is caused by mutations in the fibrillin-1 gene (*FBN1*). Fibrillin-1 constitutes the core of microfibrils, which provide structural stability to extracellular matrix (ECM) and are also responsible for the elastic properties of the vessel wall.[6,7] Mutations can be classified as dominant negative (DN) or as haploinsufficient (HI), depending on the effect that the mutation has on the fibrillin-1 protein.[8] DN mutations lead to a malfolded or malfunctioning fibrillin-1 protein and thus a disturbed ECM.[9,10] HI mutations are caused by the deletion of one copy of the whole gene, degradation of the mutant protein, or nonsense-mediated decay by degradation of fibrillin-1 mRNA.[10–12] The latter mutation will lead to reduced level of wild type fibrillin-1 protein, and thus compromised functionality.[9,10] In the ECM, fibrillin-1, together with fibrillin-2, also regulates the bioavailability of transforming growth factor ß (TGF-ß) by binding this growth factor in a latent complex.[13] TGF-ß signaling is responsible for the expression of connective tissue components in the ECM.[4,13] In MFS, excessive TGF-ß signaling is observed as a result of mutated fibrillin-1 in the ECM, which is thought to be responsible for AA development.[14] Malfolded fibrillin-1 proteins, may be subjected to degradation in the endoplasmic reticulum (ER) mediated by heat shock proteins A5 (HSPA5) and 47 (HSP47).[15,16]

TGF-ß isoforms regulate transcription of ECM components such as collagen and fibrin.[4,13,17–19] By binding to cell surface TGF-ß receptors (TGFBR1, -2 and –3; TGFBR3 is also known as Betaglycan), their downstream intracellular pathway is activated by SMADS, the intracellular effectors of TGF-ß signaling.[13,19–23] SMADS are recruited to the activated receptor complex and after phosphorylation they form a complex, which is transported into the nucleus.[23] This results in the transcription of their target genes collagen type 1 alpha 1 (*COL1A1*), fibronectin (*FN1)*, *SERPINE1* and connective tissue growth factor (*CTGF*).[24–27] A negative feedback loop on the expression of TGF-ß itself is provided by the transcriptional TGF-ß target SMAD7.[19,28] TGF-ß has long been acknowledged as a major factor of MFS development, however, in the past years more studies question whether such a role can be attributed to TGF-ß.[29]

TGFBR3 is a co-receptor of the TGF-ß superfamily that increases the binding of TGF-ß to TGFBR1 and TGFBR2. In recent years however, more functions of TGFBR3 have been

identified, expanding its role from a simple co-receptor to a broader and more complex receptor. It has been suggested to influence cellular processes such as TGF-ß receptor trafficking and regulation of signaling output.[30] We hypothesized that the expression TGFBR3 may modulate TGF-ß signaling. In the current work we aimed to elucidate the role of TGFBR3 in the TGF-ß signaling pathway of MFS patients. This was investigated by the quantification of mRNA expression of *TGFBR3* and *TGFB*, as well as a panel of TGF-ß signaling-associated target genes in primary dermal fibroblasts of MFS patients. TGFBR3 expression was studied at the protein level by immunofluorescence staining in MFS fibroblasts. As the type of mutation modulates the effect on a protein level, a differentiation was made for patients with a DN and a HI *FBN1* gene mutation.[8]

2. MATERIAL AND METHODS

2.1 Patients and healthy volunteers

The study was approved by the Medical Ethical Committee of the Amsterdam University Medical Center. Primary dermal fibroblasts were cultured from skin biopsies taken from the upper arm of thirteen patients (7 men) with a median age (with range) of 37 years (9 – 64), all with a known mutation in the *FBN1* gene (4 DN and 9 HI mutations). As control fibroblasts of 10 healthy volunteers were used (7 men) with median age 34 (0 – 56). Controls were gender-matched healthy volunteers without a medical history of cardiovascular disease. Table 7.1 shows the characteristics and *FBN1* mutations of the patients and controls.

2.2 Cell culture preparation

Primary human dermal fibroblasts were cultured in Ham's F10 Nutrient Mix Medium (Thermo Fischer Scientific; catalog number 31550031) supplemented with 10% fetal bovine serum (Thermo Fischer Scientific; catalog number 10270106), 100 units/mL penicillin and 100 µg/mL streptomycin (Thermo Fischer Scientific; catalog number 15070063). The cells were maintained in a humidified incubator at 37˚C and 5% CO_2. Cells were seeded in chamber slides (Thermo Fischer Scientific; catalog number 154534) and were left to attach and establish a monolayer during five days prior to immunofluorescence.

Table 7.1. Genotypic characteristics of all 13 included patients are presented. The *FBN1* mutation type is given as haploinsufficient (HI) or dominant negative (DN).

Mutants	Age	Gender	Type	Domain	Mutation	Effect
1	37	M	HI	8Cys-4	4605T>A	Y1535X
2	17	F	HI	INTRON	1468+2T>C	retention intron 11
3	20	M	HI	NA	0-allele	NA
4	39	F	HI	INTRON	3464-6C>A	splice error insACAG and NMD
5	9	M	HI	cb-EGF45	7732C>T	Q2578X and 0-allele
6	27	M	HI	cb-EGF25	4428C>A	Y1476X
7	43	F	HI	Proline-rich	1285C>T	R429X
8	64	M	HI	cb-EGF29	5368C>T	R1790X
9	24	M	HI	cb-EGF6	1387G>T	G463X
10	50	M	DN	cb-EGF24	4291T>C	C1431R
11	56	F	DN	8Cys-4	4588C>T	R1530C
12	40	F	DN	8Cys-3	2946 C>G	C982W
13	33	F	DN	cb-EGF8	1701G>T leads to 1700_1714del	G567_Q571del

2.3 Quantification of protein expression by immunofluorescence microscopy

Cells were rinsed with phosphate buffered saline (PBS) (3 times 3 minutes at 37˚C), then fixed in 4% formaldehyde containing PBS and rinsed again in 0.05% Tween (PBST) for 3 minutes. After cell membrane permeabilization by 0.2% Triton for 10 minutes, the cells were rinsed, and incubated overnight at 4˚C with the primary antibody for TGFBR3 (dilution 1:100; sc-75411, Santa Cruz, USA). After washing, cells were incubated with the secondary antibody (dilution 1:100; Molecular Probes, USA) for 30 minutes at room temperature. Additionally, samples were incubated for 20 minutes in wheat-germ-agglutinin (WGA) Alexa 555 fluorescent probes, targeting the cell membrane glycocalyx (dilution 1:50 in PBS; Molecular Probes, USA). After staining, samples were rinsed and mounted on a glass slide using VectashieldTM mounting medium containing DAPI nuclear stain (Vector Laboratories Inc., USA) and sealed using a cover glass.

Sections were examined with a Zeiss Axiovert 200M MarianasTM inverted microscope, equipped with a motorized stage (stepper-motor) z-axis increments 0.1µm, and a turret with a DIC brightfield cube and four epifluorescence cubes, having emission in blue (DAPI for cell nuclei), green (FITC for TGFBR3), red (Cy3 for cell membrane). A cooled CCD camera (Cooke Sensicam SVGA (Cooke Co., USA), 1280 x 1024 pixels), linear over

its full dynamic range, recorded images with true 16-bit capability. The microscope, camera, and data processing were controlled by SlideBookTM software (version 5.0.1.8, Intelligent Imaging Innovations, Denver, U.S.). Fifteen images covering the whole slide per patient were taken with a 63X oil-immersion objectives (CARL ZEISS, The Netherlands).

Analysis of images was conducted by a manual operator-dependent count of TGFBR3 positive vesicles and cells, which was performed by two independent researchers (representative images are seen in figure 7.1A-D). Vesicles were defined as spherical structures that demonstrate staining for both TGFBR3 and glycocalyx from the cell membrane. Vesicles were characterized as large (>6μm) or small. Furthermore, cells were counted and distinguished into positive and negative for the presence of intracellular TGFBR3. Vesicles per cell and the ratio between TGFBR3 positive cells and total cell counts were calculated after automatic nuclei counts (performed by SlideBook TM software). No interobserver variability was found in the measurements (vesicles: p=0.69; TGFBR3 positive cells: p=1.0).

2.4 Quantification of gene expression by quantitative polymerase chain reaction

Total RNA was isolated using the NucleoSpin Triprep Kit (Macherey-Nagel, Düren, Germany). Complementary DNA synthesis was performed using the VILO kit (Macherey-Nagel, Düren, Germany), in a 20μL reverse transcription reaction, according to manufacturer's instructions. Quantitative PCR (qPCR) was performed to show the effect of the mutations on mRNA level in *FBN1* (NM_000138), and to analyze the potential effect of the mutation on the expression of related and target genes: *FBN*2 (NM_001999), *FBN*3 (NM_032447), *FN*1 (NM_002026), *SERPINE*1 (NM_000602), SMAD7 (NM_005904), *TGFB1* (NM_000660), *TGFBR1* (NM_004612), *TGFBR2* (NM_003242), *TGFBR3* (NM_003243), *COL1A1* (NM_000088), *CTGF* (NM_001901) *HSP47* (NM_001207014) and *HSPA5* (NM_005347). As housekeeping genes for the normalization of the acquired data *YWHAZ* (NM_003406), *HPRT* (NM_000194) and *UBC* (NM_021009) were used. The analysis was performed using the using the Light Cycler SYBR Green I Master (Roche Applied Science, Penzberg, Germany) in the LightCycler 480 Instrument II (Roche Applied Science, Penzberg, Germany), as described before in more detail.[31]

Each qPCR reaction was prepared in a total volume of 10μL, consisting of 2μl PCR grade water, 1μL forward primer (10pM), 1μL reverse primer (10pM) and 5μL Light Cycler Mastermix (Light Cycler 480 SYBR Green I Master; Roche Applied Science), to which 2μL of the synthesized cDNA was added. Using absolute quantification, all values were determined based on standard curve of four serial dilutions ranging from 10ng

until 0.08ng of human reference cDNA (Agilent Technologies, Santa Clara, CA). qPCR efficiency was assessed using the fit points method, and gene expression data was analyzed with the efficiency ranging between1.7-2.0. Moreover, mRNA expression of the investigated genes was normalized by a normalization factor derived from the expression of three housekeeping genes (*YWHAZ*, *HPRT* and *UBC*).

2.5 Statistical analysis

Data were analyzed with SPSS (IBM Statistics v24, Chicago, IL). For multiple groups, the Kruskal–Wallis was used first to compare continuous variables with nonparametric distribution; subsequently, the Mann–Whitney U test was used for comparing two groups. Fisher's exact test was used for categorical variables in two groups. Raw data are given in the text as median with ranges in between brackets and data are presented graphically as boxplots (showing median and quartiles) with outliers (according to Tukey's criteria) indicated separately. Correlations between two continuous variables were calculated by Spearman rank. Tests were considered statistically significant at $P<0.05$. In case of multiple testing, corrected p-values are used according to Bonferroni.

3. RESULTS

3.1 Protein expression in cell lines

By immunofluorescence microscopy, a significantly higher ratio of TGFBR3 positive cells was observed in the cell cultures of both DN and HI groups pooled (median 0.35 [0.11 - 0.80]) as compared to controls (median 0.00 [0.00 - 0.37]; p=0.004). DN patients had higher ratios of TGFBR3 positive cells (median 0.47 [0.14 – 0.80]) than HI patients (median 0.33 [0.11 – 0.80]; p=0.015). No differences were found in the expression of TGFBR3 vesicles between *FBN1* mutant cells and controls or between DN and HI patients (table 7.2 and figure 7.1).

Table 7.2. TGF-ß receptor 3 protein expression was demonstrated by immunofluorescence microscopy in membrane-encapsulated vesicles or in the endoplasmic reticulum. Vesicles were classified as small (≤ 6µm) or large. The ratio of vesicles per nucleus is given, as well as the ratio of cells positive for TGF-ß receptor 3 in the endoplasmic reticulum per total cell count. Median ratios are given with ranges in between brackets. Genetic expressions were measured by quantitative polymerase chain reaction and presented in arbitrary units. Statistical differences between *FBN1* mutants pooled and controls are given by p-values, as well as between DN and HI *FBN1* mutations. P-values <0.05 were considered significant and are indicated by an asterisk.

Immunofluorescence microscopy	**Mutants (total)**	**Control**	**p-value**	**DN**	**HI**	**p-value**
	n = 13	*n = 10*		*n = 4*	*n = 9*	
Small vesicles (per nucleus)	0.14 (0.03 - 0.60)	0.14 (0.03 - 0.30)	0.419	0.26 (0.07 - 0.41)	0.12 (0.03 - 0.60)	0.643
Large vesicles (per nucleus)	0.02 (0.00 - 0.07)	0.01 (0.00 - 0.04)	0.651	0.01 (0.00 - 0.07)	0.02 (0.00 - 0.04)	1.000
Total vesicles (per nucleus)	0.16 (0.04 - 0.61)	0.16 (0.03 - 0.30)	0.420	0.30 (0.07 - 0.41)	0.14 (0.04 - 0.61)	0.643
ß-glycan positive cells (of total)	0.35 (0.11 - 0.80)	0.00 (0.00 - 0.37)	0.004*	0.47 (0.14 - 0.80)	0.33 (0.11 - 0.80)	0.015*
Quantitative PCR	*n = 10*	*n = 6*		*n = 4*	*n = 6*	
TGFB1	7.23 (4.55 - 11.1)	4.64 (2.76 - 6.97)	0.027*	7.59 (7.19 - 11.06)	6.17 (4.55 - 7.83)	0.059
TGFBR1	1.09 (0.71 - 2.01)	1.39 (0.79 - 1.96)	0.615	1.04 (0.84 - 1.70)	1.21 (0.71 - 2.01)	0.705
TGFBR2	2.25 (1.14 - 7.95)	1.59 (0.62 - 3.75)	0.191	2.45 (1.85 - 7.95)	2.25 (1.14 - 3.11)	0.345
TGFBR3	3.65 (1.78 - 7.69)	4.33 (0.41 - 7.03)	0.688	3.21 (2.5 - 4.01)	4.74 (1.78 - 7.69)	0.257
SMAD7	7.29 (4.77 - 15.5)	5.61 (3.03 - 6.73)	0.044*	9.24 (7.09 - 15.47)	6.43 (4.77 - 11.7)	0.019*
FBN1 P1	2.08 (0.74 - 6.20)	1.83 (0.88 - 5.04)	0.546	3.48 (2.10 - 6.20)	1.93 (0.74 - 2.59)	0.014*
FBN1 P2	0.66 (0.34 - 1.25)	0.79 (0.34 - 2.12)	0.315	0.79 (0.63 - 1.25)	0.51 (0.34 - 1.21)	0.089
FBN2	8.13 (0.49 - 52.4)	11.28 (7.81 - 101.3)	0.228	8.13 (4.68 - 34.4)	8.72 (0.49 - 52.4)	0.450
HSP47	41.2 (27.9 - 75.5)	29.8 (4.56 - 50.3)	0.070	53.6 (37.5 - 75.5)	34.1 (27.9 - 51.2)	0.023*
HSPA5	2.77 (1.99 - 4.20)	2.48 (1.62 - 3.28)	0.131	2.49 (1.99 - 2.89)	3.18 (2.58 - 4.20)	0.029*
SERPINE1	42.7 (24.8 - 71.5)	35.2 (13.24 - 87.5)	0.688	51.8 (46.6 - 71.5)	39.5 (24.8 - 45.0)	0.008*
FN1	21.1 (10.4 - 64.6)	22.7 (7.61 - 33.9)	0.688	37.2 (17.5 - 64.6)	19.1 (10.4 - 27.0)	0.089
CTGF	39.5 (4.40 - 163.9)	23.6 (16.5 - 44.0)	0.615	48.5 (11.1 - 163.9)	30.2 (4.40 - 78.6)	0.571
COL1A1	1898.0 (939.0 - 2689.4)	1137.8 (406.1 - 1589.5)	0.088	2314.2 (1894.1 - 2360.0)	1269.3 (939.0 - 2689.4)	0.089

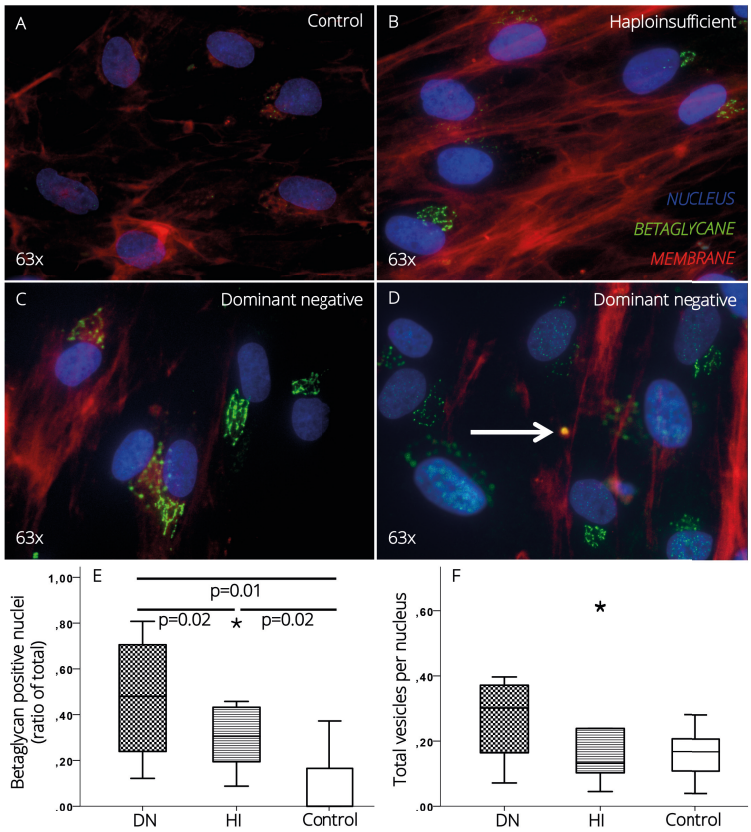

Figure 7.1 Representative immunofluorescence microscopy images of Betaglycan expression in fibroblast cell cultures of a control (A), a haploinsufficient (B) and dominant negative (C) *FBN1* gene mutation. Betaglycan was seen in the endoplasmic reticulum or in membrane encapsulated vesicles as indicated by the arrow in image D. Ratios of Betaglycan positive cells per total cell count (E) and vesicles per nucleus (F) are given as median with interquartile ranges in the boxplots. Significant differences (p≤0.05) are highlighted by a horizontal line and outliers are indicated separately by an asterisk.

3.2 Gene expression in cell cultures

By qPCR, a significantly higher gene expression was measured in *FBN1* mutant cells than in controls for both *TGFB1* (median 7.23 [4.55 - 11.1] versus 4.64 [2.76 - 6.97]; p=0.027; respectively) and *SMAD7* (median 7.29 [4.77 - 15.5] versus 5.61 [3.03 - 6.73]; p=0.044; respectively). *COL1A1* had a tendency to be higher (median 1898.0 [939.0 - 2689.4]) than in controls (median 1137.8 [406.1 - 1589.5]; p=0.088), as well *HSP47* (median 41.2 [27.9 - 75.5] versus 29.8 [4.56 - 50.3]; p=0.070, respectively). No differences were found in *TGFR1*, *-2* and *–3* expression between groups, or in downstream proteins *FBN1* and *FBN2*, HSPA5, *FN1*, *SERPIN1* and *CTGF*. See figure 7.2 for boxplots of a selection of gene expressions.

Subgroup analysis showed higher gene expressions in DN as compared to HI of *SMAD7* (median 9.24 [7.09 - 15.47] versus 6.43 [4.77 - 11.7]; p=0.019; respectively), *FBN1* P1 (median 3.48 [2.10 - 6.20] versus 1.93 [0.74 - 2.59]; p=0.014; respectively), *HSP47* (median 53.6 [37.5 - 75.5] versus 34.1 [27.9 - 51.2]; p=0.023; respectively) and *SERPIN1* (median 51.8 [46.6 - 71.5] versus 39.5 [24.8 - 45.0]; p=0.008; respectively). DN had lower gene expression of *HSPA5* than HI (median 2.49 [1.99 - 2.89] versus 3.18 [2.58 - 4.20]; p=0.029; respectively). DN tended to have higher gene expressions than HI of *TGFB1* (median 7.59 [7.19 - 11.06] versus 6.17 [4.55 - 7.83]; p=0.059; respectively), *FBN1* P2 (median 0.79 [0.63 - 1.25] versus 0.51 [0.34 - 1.21]; p=0.089; respectively) *FN1* (median 37.2 [17.5 - 64.6] versus 19.1 [10.4 - 27.0]; p=0.089; respectively) and *COL1A1* (median 2314.2 [1894.1 - 2360.0] versus 1269.3 [939.0 - 2689.4]; p=0.089; respectively).

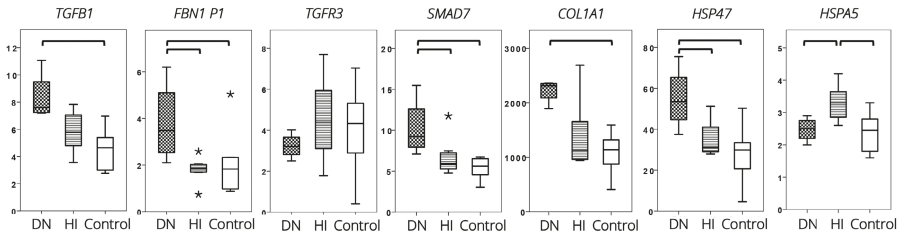

Figure 7.2 A selection of the results of quantitative polymerase chain reaction in arbitrary units in dominant negative and haploinsufficient *FBN1* mutations and controls are graphically represented as boxplots with interquartile ranges. Significant differences between groups (p≤0.05) are highlighted by an accolade. Outliers are separately indicated by an asterisk.

3.3 Correlations between protein and mRNA expression

The correlation between *TGFB1* mRNA expression with *TGFBR3* mRNA and TGFBR3 positive cells (both ratio and total positive cells) was tested (significance level after Bonferroni correction for multiple testing is p≤0.017). *TGFB1* mRNA expression was positively correlated with the ratio of TGFBR3 positive cells (Rs=0.60; p=0.017; figure 7.3). No correlation was found between TGFBR3 protein expression and *TGFBR3* mRNA expression.

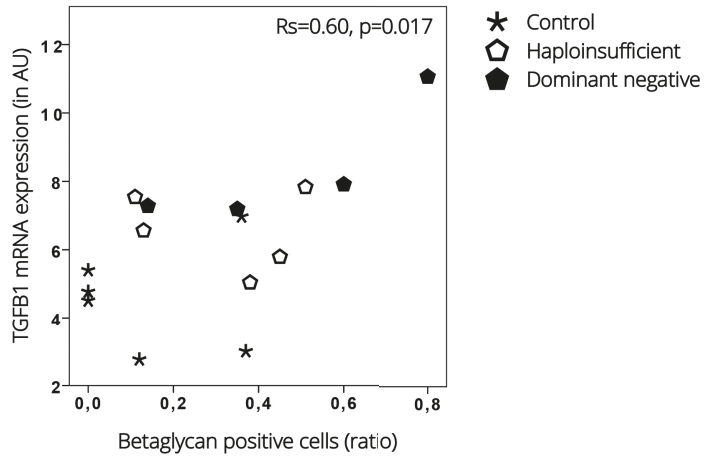

Figure 7.3 Correlations between TGFBR3 protein expression and *TGFB1* mRNA expression. The ratio of TGFBR3 positive cells to the total cell count is given on the x-axis, *TGFB1* mRNA expression on the Y-axis (in AU). Correlations are given in Spearman rank (Rs) correlation with p-value.

4. DISCUSSION

The major findings of the present study are: i) in patients with a DN *FBN1* gene mutation, fibroblasts have upregulated *TGFB1* and associated downstream signaling activation as compared to controls. Also, DN *FBN1* gene mutants have a tendency of upregulated *TGFB1* and associated signaling activation as compared to HI *FBN1* gene mutants; ii) TGFBR3 protein expression in patients with a DN *FBN1* gene mutation is higher than in the HI group; iii) *TGFB1* expression is positively correlated with TGFBR3 protein expression.

The intracellular downstream pathway of TGF-ß involves, among others, SMAD7 activation as well as transcription of COL1A1 and FN1.[20–27] In figure 7.4 we graphically represented the investigated part of the pathway in DN mutants. We demonstrated upregulated TGF-ß activation and downstream signaling. On a protein level we observed more TGFBR3 expression in DN *FBN1* gene mutants than in HI patients. It has been suggested that TGFBR3 is able to inhibit as well as enhance downstream TGF-ß signaling.[30] However, it remains a matter of debate how TGFBR3 provides the downstream TGF-ß signaling in MFS.[30] It has been acknowledged that TGFBR3 stimulates downstream signaling by presenting TGF-ß to TGFBR2.[18] Recently, however, two studies suggested that TGFBR3 regulates the signaling turnover by adjusting the ratio of soluble

to membrane bound receptors.[32,33] In the current study we demonstrated a positive correlation between TGFBR3 protein expression and TGF-ß signaling. We acknowledge that no knock-out or over-expression experiments have been performed, which hinders providing causative correlations. However, our data suggest that increased expression of TGFBR3 in MFS patients with DN mutation enhances activation of the TGF-ß signaling pathway. Our study warrants further investigation of the role of TGFBR3.

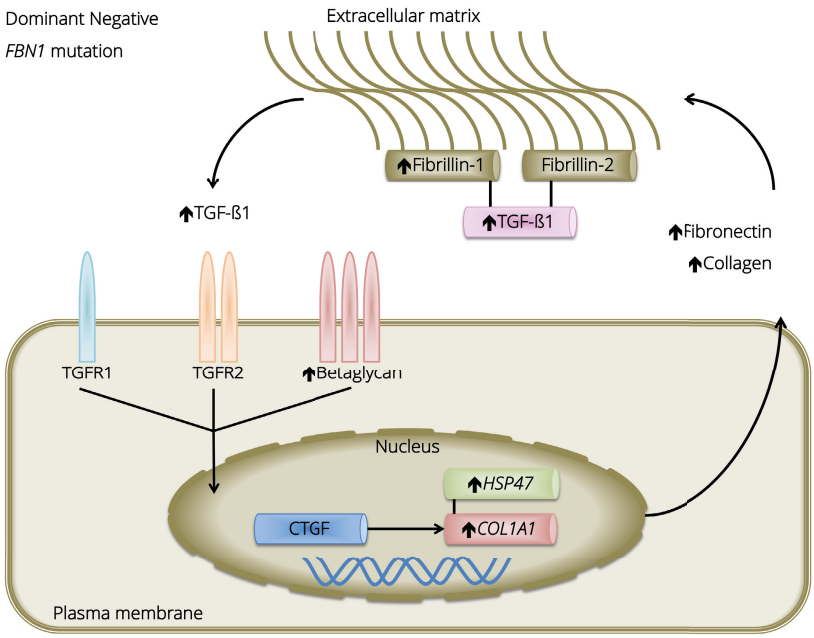

Figure 7.4 TGF-ß signaling and its partially downstream pathways in dominant negative *FBN1* mutations. Upward pointing arrows indicate increased expression as compared to healthy controls. In the extracellular matrix fibrillin-1 expression is upregulated, though it partly concerns wild type but also malfolded proteins. Therefore its binding capacity to TGF-ß1 is affected, resulting in high levels of free TGF-ß1 in the extracellular matrix. The intracellular downstream pathway of TGF-ß1 is consequently activated in higher amounts. Interestingly, increased downstream activation occurs while the amount of TGF-ß receptors are similar to controls. Eventually, intranuclear transcription of COL1A1 and its chaperone protein HSP47 are upregulated resulting in increased collagen expression and the tendency of higher fibronectin expression.

TGFBR3 protein expression was observed in two distinct locations in the cell, either in the ER or in intracellular membrane encapsulated vesicles. We observed higher expressions of TGFBR3 in MFS patients with a DN than a HI mutation. However, no differences were found in gene expression of *TGFBR3* between mutants and controls or between DN and HI. We hypothesize that the encapsulated TGFBR3 is stored in vesicles in order to regulate the total amount of receptors that are expressed on the

cell membrane. By doing so, as described above, TGFBR3 might adjust the ratio of soluble to membrane bound receptors and influence TGF-ß signaling.[33] This hypothesis could explain the discrepancy between *TGFBR3* mRNA and TGFBR3 protein expression in fibroblasts. However, one must realize that we investigated cell cultures of skin fibroblasts that lack an ECM like in the aortic wall. The lack of ECM might alter the stimulation and direction of the TGFBR3 filled vesicles.

As discussed earlier, fibrillin-1 protein is involved in the regulation of TGF-ß bioavailability in the ECM by binding to complexes of latent TGF-ß.[13] In patients with a DN *FBN1* mutation we observed upregulated *FBN1* gene expressions as compared to controls and a tendency of higher expressions in the DN than in the HI group. In MFS patients with a DN mutation this will lead to malfunctioning fibrillin-1 protein, with less capacity to bind latent TGF-ß in the ECM.[9] We suggest that in DN *FBN1* gene mutants this might be the cause of increased free TGF-ß in the ECM of diseased vessel walls, as was earlier demonstrated.[34] Fibrillin-2 protein has also been acknowledged to have a role in the regulation of free TGF-ß in the ECM.[13] However, we found that TGF-ß and its downstream signaling was increased in DN mutants, despite similar *FBN2* gene expression. Therefore, we suggest that fibrillin-2 has only a limited role in the level of TGF-ß expression.

A remarkable contradiction was the finding of upregulated expression of *HSP47* in the DN group as compared to HI patients, versus downregulated expression of *HSPA5* in the DN group as compared to HI patients. Both genes are acknowledged as ER stress markers, more specifically as markers of activated unfolded protein response.[35,36] Furthermore, TGF-ß has been demonstrated to upregulate the expression of *HSP47*.[37] Therefore, increased *HSP47* expression was expected in the DN group, as DN *FBN1* mutations lead to malfolded fibrillin-1 proteins and consequently to activation of the unfolded protein response. We did not expect *HSPA5* expression to be increased in the HI group as compared to the DN group and controls. This could be explained by the fact that HSPA5 also functions as a chaperone protein, transporting newly synthesized polypeptides and facilitates their assembly into proteins. This process may be disturbed in DN mutants.[15,16]

The use of fibroblasts may be regarded as a limitation of this study, as it possibly does not fully reflect aortic cell pathology. These cells have the genotype but not the phenotype. However, it has been demonstrated that patients with enhanced TGF-ß signaling in dermal fibroblasts also are associated with multiple syndromic presentations of aortic aneurysms.[38] We therefore consider these cells to be representative for this part of the investigated pathway. Furthermore, in the current work we have mainly focused

on the genetically stimulation. Therefore, at this time our data lack clinical information. Therefore, our model does not take into account the potential impact of aspects such as phenotypic variation between patients and pharmacological treatments.

The implication of the present work is that it emphasizes important differences in patients between the effects of DN versus HI mutations of the *FBN1* gene. A recent study showed that MFS patients with HI *FBN1* mutations had higher therapeutic benefit from Losartan treatment compared to patients with DN *FBN1* mutations which indicates a distinct pathological mechanism.[8] Thus, the different types of *FBN1* mutations must be approached in a different manner in the search for therapeutic options.

In conclusion, we demonstrated an increased activation of TGF-ß and its downstream signaling pathway in patients with a DN *FBN1* gene mutation as compared to patients with a HI *FBN1* mutation and to control groups. Also, TGFBR3 protein expressions are increased in the DN group and correlate positively with *TGFB1* expressions in groups pooled. We suggest that TGFBR3 expression is involved in upregulated TGF-ß signaling in MFS patients with a DN *FBN1* gene mutation.

REFERENCES

1. Dietz HC. Marfan syndrome. In: *Marfan Syndrome. 2001 Apr 18 [Updated 2017 Feb 2]. In: Pagon RA, Adam MP, Ardinger HH, et Al., Editors. GeneReviews® [Internet]. Seattle (WA): University of Washington, Seattle; 1993-2017.* https://www.ncbi.nlm.nih.gov/books/NBK1335/.
2. Takeda N, Yagi H, Hara H, et al. Pathophysiology and Management of Cardiovascular Manifestations in Marfan and Loeys-Dietz Syndromes. *Int Heart J*. 2016:271-277. doi:10.1536/ihj.16-094.
3. Sakai LY, Keene DR, Renard M, De Backer J. FBN1: The disease-causing gene for Marfan syndrome and other genetic disorders. *Gene*. 2016;591(1):279-291. doi:10.1016/j.gene.2016.07.033.
4. Gillis E, Van Laer L, Loeys BL. Genetics of thoracic aortic aneurysm: At the crossroad of transforming growth factor-β signaling and vascular smooth muscle cell contractility. *Circ Res*. 2013;113(3):327-340. doi:10.1161/CIRCRESAHA.113.300675.
5. Attenhofer Jost CH, Greutmann M, Connolly HM, et al. Medical treatment of aortic aneurysms in Marfan syndrome and other heritable conditions. *Curr Cardiol Rev*. 2014;10(2):161-171. doi:10.2174/1573403X1002140506124902.
6. Zeyer KA, Reinhardt DP. Engineered mutations in fibrillin-1 leading to Marfan syndrome act at the protein, cellular and organismal levels. *Mutat Res - Rev Mutat Res*. 2015;765:7-18. doi:10.1016/j.mrrev.2015.04.002.
7. Jensen S, Handford P. New insights into the structure, assembly and biological roles of 10-12 nm connective tissue microfibrils from fibrillin-1 studies. *Biochem Jounal*. 2016;473(7):827-838. doi:10.1042/BJ20151108.
8. Franken R, Den Hartog AW, Radonic T, et al. Beneficial Outcome of Losartan Therapy Depends on Type of FBN1 Mutation in Marfan Syndrome. *Circ Cardiovasc Genet*. 2015;8(2):383-388. doi:10.1161/CIRCGENETICS.114.000950.
9. Faivre L, Collod-Beroud G, Loeys BL, et al. Effect of Mutation Type and Location on Clinical Outcome in 1,013 Probands with Marfan Syndrome or Related Phenotypes and FBN1 Mutations: An International Study. *Am J Hum Genet*. 2007;81(3):454-466. doi:10.1086/520125.
10. Hilhorst-Hofstee Y, Hamel BCJ, Verheij JBGM, et al. The clinical spectrum of complete FBN1 allele deletions. *Eur J Hum Genet*. 2011;19(3):247-252. doi:10.1038/ejhg.2010.174.
11. Schrijver I, Liu W, Odom R, et al. Premature Termination Mutations in FBN1: Distinct Effects on Differential Allelic Expression and on Protein and Clinical Phenotypes. *Am J Hum Genet*. 2002;71(2):223-237. doi:10.1086/341581.
12. Schrijver I, Liu W, Brenn T, Furthmayr H, Francke U. Cysteine substitutions in epidermal growth factor-like domains of fibrillin-1: distinct effects on biochemical and clinical phenotypes. *Am J Hum Genet*. 1999;65(4):1007-1020. doi:10.1086/302582.
13. Ten Dijke P, Arthur HM. Extracellular control of TGFβ signalling in vascular development and disease. *Nat Rev Mol Cell Biol*. 2007;8(11):857-869. doi:10.1038/nrm2262.
14. Habashi JP, Judge DP, Holm TM, et al. Losartan, an AT1 antagonist, prevents aortic aneurysm in a mouse model of Marfan syndrome. *Science (80-).* 2006;312(5770):117-121. doi:10.1126/science.1124287.
15. Zhu G, Lee AS. Role of the unfolded protein response, GRP78 and GRP94 in organ homeostasis. *J Cell Physiol*. 2015;230(7):1413-1420. doi:10.1002/jcp.24923.

16. Morry J, Ngamcherdtrakul W, Gu S, et al. Dermal delivery of HSP47 siRNA with NOX4-modulating mesoporous silica-based nanoparticles for treating fibrosis. *Biomaterials*. 2015;66:41-52. doi:10.1016/j.biomaterials.2015.07.005.

17. López-Casillas F, Payne HM, Andres JL, Massagué J. Betaglycan can act as a dual modulator of TGF-β access to signaling receptors: Mapping of ligand binding and GAG attachment sites. *J Cell Biol*. 1994;124(4):557-568. doi:10.1083/jcb.124.4.557.

18. López-Casillas F, Wrana JL, Massagué J. Betaglycan presents ligand to the TGFß signaling receptor. *Cell*. 1993;73(7):1435-1444. doi:10.1016/0092-8674(93)90368-Z.

19. Massagué J, Gomis RR. The logic of TGFβ signaling. *FEBS Lett*. 2006;580(12):2811-2820. doi:10.1016/j.febslet.2006.04.033.

20. Hill CS. Nucleocytoplasmic shuttling of Smad proteins. *Cell Res*. 2009;19(1):36-46. doi:10.1038/cr.2008.325.

21. Heldin C, Moustakas A. Signaling Receptors for TGF- b Family Members. *Cold Spring Harb Perspect Biol*. 2016;8(8). doi:10.1101/cshperspect.a022053.

22. Xie S, Sukkar MB, Issa R, Oltmanns U, Nicholson AG, Chung KF. Regulation of TGF-ß1-induced connective tissue growth factor expression in airway smooth muscle cells. *Am J Physiol Lung Cell Mol Physiol*. 2005;288:68-76. doi:10.1152/ajplung.00156.2004.

23. Feng X-H, Derynck R. Specificity and Versatility in Tgf-B Signaling Through Smads. *Annu Rev Cell Dev Biol*. 2005;21(1):659-693. doi:10.1146/annurev.cellbio.21.022404.142018.

24. Lindahl GE, Chambers RC, Papakrivopoulou J, et al. Activation of fibroblast procollagen α1(I) transcription by mechanical strain is transforming growth factor-ß-dependent and involves increased binding of CCAAT-binding factor (CBF/NF-Y) at the proximal promoter. *J Biol Chem*. 2002;277(8):6153-6161. doi:10.1074/jbc.M108966200.

25. Pan X, Chen Z, Huang R, Yao Y, Ma G. Transforming Growth Factor β1 Induces the Expression of Collagen Type I by DNA Methylation in Cardiac Fibroblasts. *PLoS One*. 2013;8(4). doi:10.1371/journal.pone.0060335.

26. Ignotz RA, Massagué J. Transforming growth factor-beta stimulates the expression of fibronectin and collagen and their incorporation into the extracellular matrix. *J Biol Chem*. 1986;261(9):4337-4345. http://www.ncbi.nlm.nih.gov/pubmed/3456347.

27. Dallas SL, Sivakumar P, Jones CJP, et al. Fibronectin regulates latent transforming growth factor-β (TGFβ) by controlling matrix assembly of latent TGFβ-binding protein-1. *J Biol Chem*. 2005;280(19):18871-18880. doi:10.1074/jbc.M410762200.

28. Yan X, Liu Z, Chen Y. Regulation of TGF-beta signaling by Smad7. *Acta Biochim Biophys Sin (Shanghai)*. 2009;41(4):263-272. doi:10.1093/abbs/gmp018.Review.

29. Akhurst RJ. The paradoxical TGF-β vasculopathies. *Nat Genet*. 2013;44(8):838-839. doi:10.1002/ana.22528.Toll-like.

30. Bilandzic M, Stenvers KL. Betaglycan: A multifunctional accessory. *Mol Cell Endocrinol*. 2012;359(1-2):13-22. doi:10.1016/j.mce.2012.03.020.

31. Yeung KK, Bogunovic N, Keekstra N, et al. Transdifferentiation of Human Dermal Fibroblasts to Smooth Muscle-Like Cells to Study the Effect of *MYH11* and *ACTA2* Mutations in Aortic Aneurysms. *Hum Mutat*. 2017. doi:10.1002/humu.23174.

32. Derynck R, Zhang YE. Smad-dependent and Smad-independent pathways in TGF-β family signalling. *Nature*. 2003;425(6958):577-584. doi:10.1038/nature02006.

33. Elderbroom JL, Huang JJ, Gatza CE, et al. Ectodomain shedding of TßRIII is required for TßRIII-mediated suppression of TGF-ß signaling and breast cancer migration and invasion. *Mol Biol Cell*. 2014;25(16):2320-2332. doi:10.1091/mbc.E13-09-0524.

34. Chaudhry SS, Cain SA, Morgan A, Dallas SL, Shuttleworth CA, Kielty CM. Fibrillin-1 regulates the bioavailability of TGFβ1. *J Cell Biol*. 2007;176(3):355-367. doi:10.1083/jcb.200608167.

35. Wang J, Lee J, Liem D, Ping P. HSPA5 Gene encoding Hsp70 chaperone BiP in the endoplasmic reticulum. *Gene*. 2017;618:14-23. doi:10.1016/j.gene.2017.03.005.

36. Kawasaki K, Ushioda R, Ito S, Ikeda K, Masago Y, Nagata K. Deletion of the collagen-specific molecular chaperone Hsp47 causes endoplasmic reticulum stress-mediated apoptosis of hepatic stellate cells. *J Biol Chem*. 2015;290(6):3639-3646. doi:10.1074/jbc.M114.592139.

37. Martelli-Junior H, Cotrim P, Graner E, Sauk JJ, Coletta RD. Effect of Transforming Growth Factor-ß1, Interleukin-6, and Interferon-γ on the Expression of Type I Collagen, Heat Shock Protein 47, Matrix Metalloproteinase (MMP)-1 and MMP-2 by Fibroblasts from Normal Gingiva and Hereditary Gingival Fibromatosis. *J Periodontol*. 2003;74(3):296-306.

38. Doyle AJ, Doyle JJ, Bessling SL, et al. Mutations in the TGF-β Repressor SKI Cause Shprintzen-Goldberg Syndrome with Aortic Aneurysm. *Nat Genet*. 2013;44(11):1249-1254. doi:10.1038/ng.2421. Mutations.